Methylene Orange and Methyl Blue Adsorption Behavior on Pine Leaves Biomass (Pinus kesiya)

Phuong Thao Huynh
Dalat University
Duy-Khoi Nguyen
Duy Tan University
Bich-Ngoc Duong
Nguyen Tat Thanh University
Phi-Ho Nguyen
Dalat University
Van-Phuc Dinh (dvphuc@ntt.edu.vn)
Nguyen Tat Thanh University

Research Article

Keywords: Methylene Blue, Methyl Orange, Pinus kesiya, biosorption, heat-treatment

Posted Date: March 13th, 2023

DOI: https://doi.org/10.21203/rs.3.rs-2642269/v1

Abstract

The uptake of Methyl Orange (MO) and Methylene Blue (MB) from aqueous solutions onto Pine leaves (Pinus kesiya) was investigated in this work. Factors including pH solution, contact time, initial dye concentration were discovered to be relevant in the removal of dyes. Among four isotherm models (Langmuir, Sips, Freundlich, and Temkin), the experimental data was fitted the Langmuir model better than others. For MO and MB, the maximum Langmuir adsorption capacities were 136.99 mg.g $^{-1}$ and 140.85 mg.g $^{-1}$, respectively. The kinetic studies demonstrated that the biosorption of MO and MB onto biomass of pine leaves was compatible with Elovich, pseudo-first-order, pseudo-second-order and intra-particle diffusion models. The thermodynamic studies showed that the uptake of the two dyes was regulated by physisorption, spontaneous, and endothermic in nature. Electrostatic interactions, as well as other non-covalent forces such as π–π interactions and hydrogen bonds, are mechanisms of dyes adsorption on pine leaf biomass. The current study found that pine leaves (Pinus kesiya) might be a potential biosorbent for the wastewater treatment due to their high availability and production, resulting in various environmental advantages.

1. Introduction

It is well-known that the garment industry business is one of the most polluting industries on the planet. Sewing factories contribute one-fifth of all industrial water pollution in the world and utilize 20,000 chemicals, many of which are carcinogenic. Textile manufacturing causes for approximately 20% of global clean water contamination from colored and finished goods. Contaminated fiber dyeing waste liquid contains heavy metals and organic compounds that are difficult to break down and a pH range of 9 to 12. Many harmful chemicals are employed in the dye manufacturing process, including dyes, surfactants, electrolytes, emulsifiers, media, starches, yeasts, and oxidants. When these chemicals are thrown improperly, they can harm nearby bacteria, fish, and aquatic creatures. These pollutants can also permeate the soil, remain there for extended periods, harm groundwater supplies, and endanger human life. Furthermore, textile-dyed wastewater is highly colored, often varies depending on the kind of dye, and has a high temperature, so it must be adequately cleaned before release to avoid environmental damage (Zhou et al. 2019).

The removal of colorants from wastewater has faced many significant disadvantages, such as high costs, hazardous product production, and high energy needs. As a result, we must seek new solutions and create more ecologically friendly technology. Because conventional adsorbents are easy to find, easily accessible, renewable, ecologically benign, and can replace traditional adsorbents, biosorption is one of the most successful ways (Yagub et al. 2014). To date, a range of low-cost adsorbents, such as potato peel (Guechi &Hamdaoui 2015), dragon fruit leaves (Haddadian et al. 2013), pine cone (Sen et al. 2011), rice straw (Cheng et al. 2015), fly ash (Das et al. 2012),… and other materials, have been investigated. Adsorbents based on these biologics have been utilized to eliminate acidic, basic, and reactive dyes from waste water. All of these bio-wastes are common and have little monetary worth. Adsorption is extremely

reliant on the $pH_{solution}$, the dosage of the adsorbent, the temperature, and the concentration of other solutes present in the solution, according to the authors.

Pinus kesiya is popular in Southeast Asia for a range of applications such as boxes, pulp and paper, and temporary utility poles. Scientists have paid little attention to Pinus kesiya as an adsorbent to eliminate methylene blue and methyl orange from aqueous solutions, even though it is a cheap, easy-to-use, and ecologically benign material. The impact of critical adsorption factors on adsorption efficiency was examined. Isotherm, kinetic and thermodynamic analyses, as well as biomass characterization before and after the adsorption, were utilized to indicate the dye adsorption process evaluated on the generated biomass.

2. Materials And Methods

2.1. Biosorbent

The waste pine leaves collected from Dalat, Vietnam were completely cleaned by soaking in clean water for a day to eliminate adherent dust particles, prior to being washed with distilled water until the colorless rinse water. Next, they were cut approximately 2 cm before drying at 80^{o}C for 24 hours to achieve a consistent weight. The samples were baked at 300^{o}C for 2 hours after being crushed and sieved to size in a range of [125µm, 212 µm]. To eliminate humidity, the biomass was kept in airtight plastic containers, which were then used in the adsorption experiments. Pine leaves before and after the treatment were presented in Fig. 1.

2.2. Chemicals

Methylene Blue ($C_{16}H_{18}ClN_3S.3H_2O$; M.W: 373.9 g/mol; C.I. 52015) and Methyl Orange ($C_{14}H_{14}N_3O_3SNa$; M.W: 327.34 g/mol; C.I.13025) were producted by MERCK. To prepare 1000 ppm stock solutions, a precise weight of MO and MB diluted in 1000 mL of distilled water was 1.000 g and 1.1690 g, respectively. These lower concentration solutions were created by diluting stock solutions. pH of solutions was adjusted with 0.1000 M HCl and NaOH solution and measured with Inolab 730.

2.3. Determination of point of zero charge

Prepared 10 flasks containing 50 mL of 0.1 M KCl solution with the corresponding pH_i values adjusted from 2 to 11. Added 0.1 g of material to the flasks prepared above, covered and stirred for 24 hours. Then, filtered the solution and measured the pH value (called pH_f). Determined the graph of dependency ΔpH ($\Delta pH = pH_i - pH_f$) on pH_i. The zero charge point of the material (pH_{pzc}) was the intersection pointed between the plot and the Ox axis at the value ΔpH = 0. Carried out the test three times for each pH_i value of the solution.

2.4. Adsorption experiments

Effects of factors, such as pH (2–10), starting dye concentration (100–500 $mg.L^{-1}$), and contact duration (10–240 min) on the biosorption of MB and MO were examined and conducted in triplicate in batch. Herein, 0.1 g of pine leaves biomass was placed to 50 mL capped glass bottles containing 100 $mg.L^{-1}$ of dye solutions. Shake the solution at 150 rpm at room temperature (25 ^0C). After the adsorption, the mixture was filtered on the filter paper to get the solution. The residual concentration of the dye in the supernatant was determined by a UV–Vis spectrophotometer at a wavelength maximum of 665 nm and 465 nm for the MB and MO, respectively.

The adsorption capacity and efficiency are determined as follows:

$$q_e = \frac{(C_0 - C_e)V}{m} \quad (1)$$

$$H\% = \frac{(C_0 - C_e).100\%}{C_0} \quad (2)$$

Where C_0 and C_e are concentrations of dye before and after the adsorption ($mg.L^{-1}$), respectively. q_e is the adsorption capacity ($mg.g^{-1}$). V represents the volume (L) of the solution, and m is the mass of biosorbent utilized (g).

2.5. Kinetic studies

To evaluate physiochemical interactions between biomass and dyes, the nature of sorption process, and rate-limiting step, all of which play an vital role for the design of commercial sorption systems, adsorption kinetic modeling is fitted with experimental data to determine kinetic parameters. As a consequence, the nonlinear equations (pseudo-first-order, pseudo-second-order, Elovich, and intra-diffusion models) were used to fit adsorption kinetic models to the biomass kinetic study data as shown in Supplemental Information.

2.6. Adsorption studies

Using equilibrium isotherm modeling plays an instrumental role in determining the distribution of dye molecules on the biomass surface, leading to an understanding of the dye-biomass adsorption mechanism. For this study, four isotherm models (Langmuir, Freundlich, Sips, Temkin) were fitted with experimental data to examine the sorption processes of cationic and anionic dyes onto the biomass. The fomulars and meanings of these models were shown in Supplemental Information.

2.7. Adsorption thermodynamics

Thermodynamic investigations of the biosorption of dyes onto biomass of pine leaves were carried out at various temperatures (298–328 K). The following equations may be used to calculate parameters consisting of enthalpy changes (ΔH^0: $KJ.mol^{-1}$), entropy changes (ΔS^0: $J\ mol^{-1}.K^{-1}$) and free energy changes (ΔG^0: $KJ.mol^{-1}$):

$$\Delta G^0 = -RT\ln K_C \quad (11)$$

$$\Delta G^0 = \Delta H^0 - T.\Delta S^0 \quad (12)$$

$$\ln K_C = \frac{\Delta H^0}{RT} - \frac{\Delta S^0}{R} \quad (13)$$

Where R represents the universal gas constant (8.314 $J.mol^{-1}.K^{-1}$), T represents the absolute temperature (Kelvin), and K_C represents the equilibrium adsorption constant. The dye's ΔH^0 and ΔS^0 values were derived using the slope and intercept of the LnK_C vs 1/T plot, respectively. The data utilized in the preceding study are all mean values from three replicate experiments.

3. Results And Discussion

3.1. Characterization of adsorbents

Figure 2 depicted the material's surface as coarse, porous, and riddled with holes. The sizes of the holes were quite uniform that facilitated the adsorption process. This material had many holes so the adsorption process took place and achieved good adsorption efficiency in a short time. The S4800 Field Emission Scanning Electron Microscope was applied for visualize morphological features on the surface of materials (Hitachi, Japan).

The EDX spectrossic examination revealed that the primary components of the substance were carbon and oxygen at a volume rate of 66.47% and 33.53%, respectively. The above ratio was due to the activation of the material at 300^0C – this process helped to convert organic compounds found in the leaves such as Lignin, Holocellulose, etc. into gases. These gases flew away leaving blanks, which was the porosity mechanism that facilitated the adsorption process.

Pine leaves are mostly made of cellulose and lignin, whose components serve as active sites for dye adsorption. To determine the active functional group on the surface of materials, FT-IR spectra of pine leaf biomass before and after dye adsorption were determined by Nicolet iS5 FT-IR spectrometer (Thermo Fisher, USA) and shown in Fig. 3. The spectra presented many peaks, indicating that pine leaves contain a variety of functional groups that may aid in the binding of dye molecules.

The absorbance bands of pine leaves biomass were discovered to comprise a large overlapping band at 3200–3500 cm^{-1}, with a peak at 3412 cm^{-1}, which can be attributed to hydroxyl group O-H stretching and intermolecular hydrogen bonding. This band's location and asymmetry suggested the presence of strong hydrogen bonds. This peak diminished following dye adsorption, showing that the O-H and hydrogen bonds in pine leaves biomass were disrupted in order to react with dye.

The signal at 2955 cm^{-1} indicates vibration of CH_n, mainly owing to C-CH_2 and C-CH bonds, whereas a peak of 1735 cm^{-1} presents the C = O group of the carbonyl in the hemicellulose (Zhu et al. 2016). The existence of C = C stretching of the phenol group is shown by the peaks at 1600 cm^{-1}. Whereas peaks at 1033 cm^{-1} in the spectrum lead to a strong C-O bond due to the cellulose ether group (Silva et al. 2019).

Except for minor differences, the spectra of the dye-loaded pine leaves biomass exhibited comparable properties to the adsorbent in natural form. After the adsorption, the specific peaks are somewhat moved from their original positions, and the intensity changes. These findings indicated that functional groups contribute the adsorption of dye ions of the pine leaves biomass via weak electrostatic contact or Van der Waals interactions.

3.1. Survey results of zero charge point (pH_{pzc}) and effect of pH on Dyes Adsorption

The pH_{pzc} value was about 7.5 based on the material's zero-charge graph. This finding allowed us to anticipate the material's adsorption capability for MB and MO at any pH value. When the pH of the solution was less than 7.5, the material's surface was positively charged, and excellent anion adsorption was favored. If the solution pH was more than 7.5, the material's surface would have a negative charge and improved cation adsorption (Banerjee &Chattopadhyay 2017). This was the basis of investigating the factors influencing pH on adsorption capacity to determine the optimal pH value of MB and MO.

Figure 5a depicts the fluctuation of MB and MO adsorption capabilities on biomass at various pH levels. From this figure, the adsorption capacity of MO rose as the pH value decreased, but the uptake of MB showed to the contrary. Clearly, the adsorption capacity of biomass towards MB and MO is significantly reliant on solution pH because it impacts the speciation of the dye as well as the adsorbent's surface charge distribution in the solution. In other words, it might affect the electrostatic interactions of an attracting or repulsive nature between the dye species in the solution and the surface of the biomass of pine leaves.

Noticeably, there was a tendency to increase the adsorption capacity of MB from pH = 2 to 8, prior to equilibrium at pH > 8. When dissolved in water, MB, a base-cationic dye, decomposed into MB^+ ions, and the lower the pH value (greater concentration of H^+ in the solution), the adsorption competition between MB^+ and H^+ lowered the material's MB adsorption capacity (Khnifira et al. 2022). Furthermore, carbonyl groups (C = O) and hydroxyl groups (O-H) on the adsorbent's surface can bind cationic dye molecules at the high pH. As a result, the biomass of pine leaves has a high MB adsorption capability in an alkaline environment (Yagub et al. 2012).

The adsorption of MO onto biomass reduced from 40.28 to 35.50 $mg.g^{-1}$ when the pH climbed from 2 to 10, indicating that anionic dye adsorption onto pine leaves is pH-dependent and preferential under acidic conditions. The increased anionic dye adsorption at lower pH levels has been linked to the full protonation of the biomass surface functions, which provides strong electrostatic attraction to the MO

dye molecules, allowing the dye to be quickly absorbed (Zubair et al. 2017). In contrast, increasing the pH causes an increase in anion OH^- in the solution, which competes with anionic dye molecules, resulting in a drop in the q_e of MO on biomass. This shows that electrostatic and chemical interactions were predominantly responsible for the uptake of anionic dyes onto pine leaf biomass (Zubair et al. 2020).

In order to understand how pH affects adsorption behavior, the zeta potential of the adsorbent was measured at various pH values. As demonstrated in Fig. 4, when the pH was less than 7.5, the biomass's surface potential was positive, and the uptake of anion MO was improved due to electrostatic attraction. In contrast, the surface potential of biomass was negative, which was suitable for the uptake of cation MB. However, the adsorption capacity of MB was not diminished when the pH value is higher than 9. It indicates that the adsorption mechanism of MB follows not only electrostatic interaction but also hydrogen bonding between adsorbent and adsorbate. The biomass may be considered an H-donor, whereas MB was an H-acceptor. This mechanism can also occur during MO adsorption.

According to the foregoing explanations, the optimal pH value of the material's MB and MO adsorption processes was 8 and 6. The study's findings were aligned with the findings of establishing the material's point of zero charges. Previous research has also observed similar behavior (Alseddig et al. 2017, Yang et al. 2018). Furthermore, based on Fig. 5a, it was inferred that the adsorption capacity of MB was larger than the adsorption capacity of MO at the ideal pH value. The degree of diffusion was governed by the size or shape of the molecule in organic dyes with complicated and bulky structures, such as MB and MO. To describe dye adsorption capability, use the structure and molecular weights of dyes (Sun et al. 2022).

3.3. Effect of contact time and the initial dyes concentration

Because the contact duration of the dyes biomass adsorption process was a significant factor in the adsorption system design, Fig. 5b depicts the effects of adsorption time on the adsorption capacity of anionic and cationic dyes.

According to these curves, the adsorption of the molecules of MB and MO on the pine leaves is quick during the first 60 min to reach the equilibrium, which is 150 min for the MB and MO with maximum adsorbed amounts of 44.27 $mg.g^{-1}$ and 40.97 $mg.g^{-1}$, respectively. The quick adsorption rate of the initial phase (fast phase) may be explained by the reality that he adsorption sites on the surface of our adsorbent are free at the start of the phenomenon. Once the dye molecules are immobilized, they block the pores, decreasing the rate of adsorption and resulting in a saturated array, which is why the second phase exists (slow phase). This trend is consistent with other research' conclusions (Alseddig et al. 2017, Ma et al. 2012).

At room temperature, Fig. 6a depicts the adsorption capabilities versus various starting dye concentrations. As the dye concentration rises from 100 to 500 $mg.L^{-1}$, the quantity of dye adsorbed ($mg.g^{-1}$) of both MB and MO rose from 44.28 $mg.g^{-1}$ to 127.23 $mg.g^{-1}$ (MB) and from 40.98 $mg.g^{-1}$ to 118.62 $mg.g^{-1}$ (MO). The concentration of the dye influences dye removal. The mass transfer driving

force rose as the starting concentrations increased, as did the interaction between dyes and adsorbent, resulting in increasing adsorption capacity.

As shown in Fig. 6b, raising the initial dye concentration from 100 to 500 mg.L^{-1} reduced removal from 88.55–50.89% (MB) and 81.95–47.45%. (MO). This was discussed in detail that the adsorption capacity was complete and the adsorption efficiency was high when the concentration of MB and MO was low due to the low and constant weight of the adsorbent. Notwithstanding, the amount of MB and MO was very large at the high concentration, exceeding the number of fixed adsorption centers in the material, thus these uptake were incomplete, resulting in a decline in adsorption efficiency (Zhu et al. 2016, Zubair et al. 2020).

3.4. Adsorption mechanism of MB and MO onto biomass of pine leaves

In addition to taking into account kinetics and isotherms models, as well as the characterisation of wasted biomass following the uptake of the dye, the mechanism of interaction of anionic and cationic dye molecules with biochar surface was further studied. The discussion of the findings is in the section below.

3.4.1. Adsorption equilibrium

Adsorption isotherms display the distribution of adsorbent molecules between the liquid and solid phases when the uptake obtains equilibrium. Normally, an appropriate model can be determined by fitting experimental data with several isotherm models, such as Langmuir, Freundlich, Sips, and Temkin (Ertugay &Malkoc 2014). The fitted plots from each isotherm for the adsorption of MB and MO onto biomass of *Pinus kesiya* were displayed in Fig. 7. Table 1 reports the isotherm parameters discovered via non-linear regression analysis.

Table 1
Calculated parameters (± SD) for MB and MO biosorption by Pinus kesiya biomass in single systems, acquired by non-linear regression analysis

Models	Parameters	MB	MO
Langmuir	K_L ($L.mg^{-1}$)	0.0268 ± 0.0061	0.0228 ± 0.0031
	q_{max} ($mg.g^{-1}$)	150.67 ± 8.73	142.72 ± 5.13
	R^2	0.9937	0.9981
Freundlich	n	3.35 ± 0.60	3.10 ± 0.40
	K_F ($L^n.g$)	26.41 ± 6.95	21.27 ± 4.44
	R^2	0.9872	0.9939
Sips	q_s ($L.g^{-1}$)	1.88 ± 2.90	2.31 ± 2.05
	α_s ($L.mg^{-1}$)	0.0133 ± 0.0193	0.0168 ± 0.0136
	β_s	1.22 ± 0.44	1.10 ± 0.25
	R^2	0.9930	0.9979
Temkin	K_T ($L.mg^{-1}$)	0.3298 ± 0.1675	0.2508 ± 0.0724
	b_T ($J.mol^{-1}$)	81.07 ± 11.45	82.49 ± 7.02
	R^2	0.9913	0.9971

The Langmuir adsorption model explains the MB and MO dye adsorption on the biomass of pine leaves reasonably well. The Langmuir model's coefficients of determination (R^2) for the MB and MO biosorption data (R^2 = 0.9937 for MB and R^2 = 0.9981 for MO) were greater than those for the other models. It was discovered that biomass has a maximum adsorption capacity of 150.67 $mg.g^{-1}$ (MB) and 142.72 $mg.g^{-1}$ (MO), confirming physical monolayer adsorption. The homogeneous distribution of active sites on the adsorbent surface, which is implied by the Langmuir equation, maybe the reason why the Langmuir isotherm closely matches the experimental results (Sen et al. 2011).

According to the nonlinear Freundlich isotherm, determining the constant K_F ($L^n.g$) and n coefficient (Table 1*)*. This coefficient between 1 and 10 was a favorable range for the biosorption process. This proved that pine leaves (*Pinus kesiya)* were good biosorbent materials for MB and MO in an aqueous solution.

Additionally, the Temkin model's energy values bT calculations were less than 8 kJ/mol, which supported the idea that these adsorbents underwent physical adsorption at the measured temperatures.

Table 2
The maximum adsorption capacity of MB and MO calculated from the Langmuir model using various biosorbents.

Source of adsorbents	Adsorbent	q_{max} ($mg.g^{-1}$)	Reference
Millettia thonningii seed pods	MB	14.09	(Jasper et al. 2020)
Casuarina equisetifolia pines	MB	41.35	(Chandarana et al. 2021)
Peanut shells	MB	67.42	(Benjelloun et al. 2022)
Walnut shells	MB	101.43	(Benjelloun et al. 2022)
Potato *(Solanum tuberosum)* peel	MB	105.26	(Guechi &Hamdaoui 2015)
Pine leaves	MB	150.67	This study
Corn leaves	MO	13.85	(Fadhil &Eisa 2019)
Dragon fruit foliage	MO	17.67	(Haddadian et al. 2013)
Pineapple leaf	MO	47.62	(Kamaru et al. 2015)
Populous leaves	MO	90.44	(Shah et al. 2021)
Shaddock peels-	MO	94.59	(Tao et al. 2019)
Pine leaves	MO	142.72	**This study**

The data in Table 2 compares the adsorption capabilities of several biosorbents that have been previously reported in the literature to those of pine leaves. The Pinus kesiya biomass that was presented in this study functioned superbly, outperforming the majority of other comparable adsorbents that had previously been described. As a result, pine leaves provide MB and MO from an aqueous solution a potential, cost-effective biosorbent.

3.4.2. Adsorption kinetics

In order to evaluate the effects of adsorption time on the uptake as well as the potential processes involved in removal, kinetic models were investigated (Villabona-Ortíz et al. 2022). Figure 8 depicts the fitting of experimental data to the pseudo-first-order, pseudo-second-order, Elovich, and intra-particle diffusion models using non-linear regressions.

Both cationic and anionic dyes were shown to quickly bind to biomass in the first few minutes of exposure. There are various steps to the process. Within the first minute, the surface adsorption occurs and dye molecules were transferred from the bulk phase to the surface of biomass. After that, dyes are

injected into the pores of the material. Lastly, the equilibrium stage occurs and leads to a layered process (Jiang &Hu 2019).

Therefore, interparticle diffusion takes part in the adsorption procedure but is unable to regulate the total adsorption of dye molecules. As a result, the adsorption mechanism is driven by many mechanisms (Villabona-Ortíz et al. 2022).

The characteristics in Table 2 show that all models successfully fit the kinetics of MB and MO on biomass, with an overall $R^2 > 0.99$ (Villabona-Ortíz et al. 2022). As a result, it can be concluded that the process is regulated by chemisorption and diffusive mechanisms. Additionally, the pseudo-second-order model provided an outstanding way of determining the experimental value of q_e by that determined by the model, accurately describing the experimental data. Additionally, the fact that the intra-particle diffusion model's value of C is not zero, indicating that the sorption follows not only the intra-particle diffusion but also one or more additional diffusion processes in addition to the intra-particle diffusion (Dinh et al. 2018).

Table 2
Kinetics parameters on the uptake of MB and MO of biomass of pine leaves

Models	Parameters	MB	MO
Pseudo-first-order	k_1 (min^{-1})	0.0594 ± 0.0102	0.0697 ± 0.0148
	$q_{e,cal}$ (mg/g)	42.85 ± 1.1590	39.12 ± 1.22
	R^2	0.9991	0.9990
Pseudo-second-order	k_2 ($g.mg^{-1}.min^{-1}$)	0.0021 ± 0.0004	0.0028 ± 0.0006
	$q_{e,cal}$ (mg/g)	46.15 ± 0.98	41.92 ± 1.05
	R^2	0.9997	0.9996
Elovich	α ($mg.g^{-1}.min$)	55.54 ± 23.82	91.23 ± 42.45
	B ($mg.g^{-1}$)	0.1677 ± 0.0126	0.1991 ± 0.0145
	R^2	0.9998	0.9999
Intraparticle – diffusion	k_d ($mg.g^{-1}.min$)	1.3436 ± 0.1401	1.1347 ± 0.0471
	C	26.01 ± 1.71	25.23 ± 0.57
	R^2	0.9991	0.9999

Thus, it implies that chemisorption occurring due to chemical reactions between biomass surface functions and dye molecules may govern the sorption process of both anionic and cationic dyes on

biomass (Dinh et al. 2019, Shooto et al. 2020). There were three main processes in the adsorption of MO and MB, which are as follows: On the surface of pine leaves, there are abundant active binding sites (oxygen functionalities) for dye molecules to bind to, indicating a fast rate of dye adsorption. There are also slow rates of dye adsorption, showing diffusion of dye molecules into biomass pores, and equilibrium-stage saturation of active sites. Similar outcomes were shown (Omer et al. 2022, Zhu et al. 2018, Zubair et al. 2020).

3.4.3. Temperature Effect and Thermodynamic Parameters

The biosorption isotherm is affected by temperature because it shows the thermodynamic equilibrium between dyes in aqueous solution and dyes biosorbed on the surface of biomass. Table 3 displays the findings of a study on the impact of temperature at various temperature levels (30, 40, and 50^{o}C). The capacity of MB and MO to adsorb to biomass increased with temperature, indicating that the adsorption process was an endothermic one that occurred spontaneously (Jiang &Hu 2019).

ΔG^{o} has a negative value, and its upward trend is consistent with the temperature rise. The fact that ΔH^{o} values are all positive and show that temperature has a direct impact on adsorption behavior shows that the uptakes of both dyes are spontaneous and that thermodynamic adsorption is beneficial. As the temperature rises, the adsorption capacity should grow as well. The ΔS^{o} value was positive, indicating an increase in the degree of disorder at the interface between the dye solution and the biomass.

The ΔH^{o} value can also be utilized to look into the adsorption's chemical or physical properties. The physical purification stage is crucial for van der Waals interaction when ΔH^{o} = 20 kJ/mol. When 20 kJ/mol < ΔH^{o} < 80 kJ/mol, the electrostatic contact plays a substantial role in the physical purification process. The adsorption mechanism is mostly chemical when ΔH^{o} > 80 kJ/mol (Mosoarca et al. 2022). The biomass used in this experiment to purify MB and MO has a ΔH^{o} value that is less than 80 kJ/mol, indicating that physisorption is at play, albeit a tiny chemical reaction may help the procedure.

Table 3
Thermodynamic parameters for adsorption of MB and MO onto biomass of pine leaves

	T (K)	LnK_C	ΔG (kJ/mol)	ΔH (kJ/mol)	ΔS (J/mol.K)
MB	303	1,44	-3,64	41,11	147,46
	313	1,88	-4,90		
	323	2,45	-6,60		
MO	303	0,85	-2,14	39,74	137,98
	313	1,27	-3,30		
	323	1,83	-4,90		

4. Conclusions

In this article, pine leaves (*Pinus kesiya*) were used as the potential biomass for the adsorption of MO and MB from an aqueous solution. The initial dye concentrations, pH, and contact duration all had an impact on the MO and MB adsorption by biomass. The findings of the non-linear kinetics and isotherms fitting indicate that the pseudo-second-order and Langmuir models are more suited to describe the MB and MO's adsorption characteristics on biomass. Increased temperature is beneficial for the adsorption process, as shown by the thermodynamic parameters, which also showed that the adsorption process is a spontaneous and practical purifying procedure. Furthermore, the adsorption of both kinds of dyes has been greatly aided by the surface functional groups (C = O, C-O, and -OH) of biomass (anionic and cationic). Through a number of processes, including electrostatic attraction, hydrogen bonds, and - interactions, it was determined that the adsorption process involves both chemisorption and physisorption. As a result, it can be said that biomass has potential as an economically sound substitute for removing the dye from an aqueous solution. Methylene blue and methyl orange can be eliminated from textile dyeing effluent using the research described here.

Declarations

Ethical Approval. Not applicable

Consent to Participate. Not applicable

Consent to Publish. Not applicable

Authors Contributions. Van-Phuc Dinh and Phuong Thao Huynh designed and directed the research. Van-Phuc Dinh, Phuong Thao Huynh, Duy-Khoi Nguyen, Bich-Ngoc Duong, and Phi-Ho Nguyen conceived and planned the experiments. Van-Phuc Dinh, Phuong Thao Huynh, Duy-Khoi Nguyen, Bich-Ngoc Duong, and Phi-Ho Nguyen carried out the experiments, analysed the data, and performed the isotherm and kinetic model analyses. Van-Phuc Dinh and Phuong Thao Huynh wrote the manuscript with inputs from all authors. All authors discussed the results and contributed to the final manuscript. All authors read and approved the final manuscript.

Funding. This research was supported by a Grant-in-Aid for Scientific Research No. 09TĐ from Dalat University, Vietnam.

Competing Interests. The authors declare that they have no known competing financial interests or personal relationships that could have appeared to influence the work reported in this paper.

Availability of data and materials. Not applicable

References

1. Alseddig A, Eljiedi A, Kamari A (2017): Removal of methyl orange and methylene blue dyes from aqueous solution using lala clam (*Orbicularia orbiculata*) shell, AIP Conference Proceedings
2. Banerjee S, Chattopadhyay MC (2017): Adsorption characteristics for the removal of a toxic dye, tartrazine from aqueous solutions by a low cost agricultural by-product. Arabian Journal of Chemistry 10, S1629-S1638
3. Benjelloun M, Miyah Y, Bouslamti R, Nahali L, Mejbar F, Lairini S (2022): The Fast-Efficient Adsorption Process of the Toxic Dye onto Shells Powders of Walnut and Peanut: Experiments, Equilibrium, Thermodynamic, and Regeneration Studies. Chemistry Africa 5, 375–393
4. Chandarana H, Kumar PS, Seenuvasan M, Kumar MA (2021): Kinetics, equilibrium and thermodynamic investigations of methylene blue dye removal using Casuarina equisetifolia pines. Chemosphere 285
5. Cheng M, Zeng G, Huang D, Lai C, Wei Z, Li N, Xu P, Zhang C, Zhu Y, He X (2015): Combined biological removal of methylene blue from aqueous solutions using rice straw and Phanerochaete chrysosporium. Applied Microbiology and Biotechnology 99, 5247–5256
6. Das S, Barman S, Thakur R (2012): Removal of Methyl Orange and Mythelene Blue Dyes From Aqueous Solution Using Low Cost Adsorbent Zeolite Synthesized From Fly Ash. J Environ Sci Eng 54, 472-480
7. Dinh V-P, Le N-C, Tuyen LA, Hung NQ, Nguyen V-D, Nguyen N-T (2018): Insight into adsorption mechanism of lead(II) from aqueous solution by chitosan loaded MnO_2 nanoparticles. Materials Chemistry and Physics 207, 294-302
8. Dinh V-P, Huynh T-D-T, Le HM, Nguyen V-D, Dao V-A, Hung NQ, Tuyen LA, Lee S, Yi J, Nguyen TD, Tan LV (2019): Insight into the adsorption mechanisms of methylene blue and chromium(iii) from aqueous solution onto pomelo fruit peel. RSC Advances 9, 25847-25860
9. Ertugay N, Malkoc E (2014): Adsorption Isotherm, Kinetic, and Thermodynamic Studies for Methylene Blue from Aqueous Solution by Needles of *Pinus Sylvestris* L. Pol. J. Environ 23, 1995–2006
10. Fadhil OH, Eisa MY (2019): Removal of methyl orange from aqueous solutions by adsorption using corn leaves as adsorbent material. Journal of Engineering 25, 55-69
11. Guechi EK, Hamdaoui O (2015): Biosorption of methylene blue from aqueous solution by potato (Solanum tuberosum) peel: equilibrium modelling, kinetic, and thermodynamic studies. Desalination and Water Treatment 57, 10270-10285
12. Haddadian Z, Shavandi MA, Abidin ZZ, Razi AFl-, Ismail MHS (2013): Removal Methyl Orange from Aqueous Solutions Using Dragon Fruit (Hylocereusundatus) Foliage. Chemical Science Transactions 2, 900-910
13. Jasper EE, Ajibola VO, Onwuka JC (2020): Nonlinear regression analysis of the sorption of crystal violet and methylene blue from aqueous solutions onto an agro-waste derived activated carbon. Applied Water Science 10

14. Jiang Z, Hu D (2019): Molecular mechanism of anionic dyes adsorption on cationized rice husk cellulose from agricultural wastes. Journal of Molecular Liquids 276, 105-114
15. Kamaru AA, Sani NS, Malek NANN (2015): Raw and surfactant-modified pineapple leaf as adsorbent for removal of methylene blue and methyl orange from aqueous solution. Desalination and Water Treatment 57, 18836-18850
16. Khnifira M, Hamidi SE, M.Sadiq, Şimşek S, Kaya S, Barka N, Abdennouri M (2022): Adsorption mechanisms investigation of methylene blue on the (0 0 1) zeolite 4A surface in aqueous medium by computational approach and molecular dynamics. Applied Surface Science 572, 151381
17. Ma J, F. Y, L. Z, L. J, M. Y, J. L, Y. T, H. F, Z. Y, J. C (2012): Enhanced adsorptive removal of methyl orange and methylene blue from aqueous solution by alkali-activated multiwalled carbon nanotubes. Appl Mater Interfaces 4, 5749 – 5760
18. Mosoarca G, Vancea C, Popa S, Dan M, Boran S (2022): The Use of Bilberry Leaves (Vaccinium myrtillus L.) as an Efficient Adsorbent for Cationic Dye Removal from Aqueous Solutions Polymers 14
19. Omer A, Naeem GAE, Abd-Elhamid AI, Farahat OOM, El-Bardan AA, Soliman HMA, Nayl AA (2022): Adsorption of Crystal violet and Methylene blue Dyes using a Cellulose-based adsorbent from Sugercane bagasse: Characterization, kinetic and Isotherm studies. Journal of Materials Research and Technology
20. Sen TK, Afroze S, M. AH (2011): Equilibrium, Kinetics and Mechanism of Removal of Methylene Blue from Aqueous Solution by Adsorption onto Pine Cone Biomass of *Pinus radiata*. Water, Air, & Soil Pollution 218, 499-515
21. Shah SS, Sharma T, Dar BA, Bamezai RK (2021): Adsorptive removal of methyl orange dye from aqueous solution using populous leaves: Insights from kinetics, thermodynamics and computational studies. Environmental Chemistry and Ecotoxicology 3, 172-181
22. Shooto ND, Thabede PM, Bhila B, Moloto H, Naidoo EB (2020): Lead ions and methylene blue dye removal from aqueous solution by mucuna beans (velvet beans) adsorbents. Journal of Environmental Chemical Engineering 8, 103557
23. Silva F, Nascimento L, Brito M, Silva Kd, Jr WP, Fujiyama R (2019): Biosorption of Methylene Blue Dye Using Natural Biosorbents Made from Weeds. Materials 12, 2486
24. Sun Y, Wang T, Han C, Lv X, Bai L, Sun X, Zhang P (2022): Facile synthesis of Fe-modified lignin-based biochar for ultra-fast adsorption of methylene blue: Selective adsorption and mechanism studies. Bioresource Technology 344, 126186
25. Tao X, Wu Y, Cha L (2019): Shaddock peels-based activated carbon as cost-saving adsorbents for efficient removal of Cr (VI) and methyl orange. Environmental Science and Pollution Research volume 26, 19828-19842
26. Villabona-Ortíz Á, Figueroa-Lopez KJ, Ortega-Toro R (2022): Kinetics and Adsorption Equilibrium in the Removal of Azo-Anionic Dyes by Modified Cellulose. Sustainability 14

27. Yagub MT, Sen TK, Ang HM (2012): Equilibrium, Kinetics, and Thermodynamics of Methylene Blue Adsorption by Pine Tree Leaves. Water Air Soil Pollut 223, 5267–5282
28. Yagub MT, Sen TK, Afroze S, H.M.Ang (2014): Dye and its removal from aqueous solution by adsorption: A review. Advances in Colloid and Interface Science 209, 172-184
29. Yang L, Gao J, Liu Y, Zhang Z, Zou M, Liao Q, Shang J (2018): Removal of Methyl Orange from Water Using Sulfur-Modified nZVI Supported on Biochar Composite. Water Air Soil Pollut 229
30. Zhou Y, Lu J, Zhou Y, Liu Y (2019): Recent advances for dyes removal using novel adsorbents: A review. Environmental Pollution 252, 352-365
31. Zhu W, Liu L, Liao Q, Chen X, Qian Z, Shen J, Liang J, Yao J (2016): Functionalization of cellulose with hyperbranched polyethylenimine for selective dye adsorption and separation. Cellulose 23, 3785–3797
32. Zhu Y, Yi B, Yuan Q, Wu Y, Wang M, Yan aS (2018): Removal of methylene blue from aqueous solution by cattle manure-derived low temperature biochar. RSC Advances 8, 19917–19929
33. Zubair M, Jarrah NA, Manzar MS, Al-Harthi M, Daud M, Mu'azu ND, Haladu SA (2017): Adsorption of Eriochrome Black T from Aqueous Phase on MgAl-, CoAl- and NiFe- Calcined Layered Double Hydroxides: Kinetic, Equilibrium and Thermodynamic Studies. Journal of Molecular Liquids 230, 344-352
34. Zubair M, Mu'azu ND, Jarrah N, Blaisi NI, Aziz HA, Al-Harthi MA (2020): Adsorption Behavior and Mechanism of Methylene Blue, Crystal Violet, Eriochrome Black T, and Methyl Orange Dyes onto Biochar-Derived Date Palm Fronds Waste Produced at Different Pyrolysis Conditions. Water Air Soil Pollut, 231-240

Figures

Figure 1

Pine leaves (a) and the adsorbent after the heat treatment at 300 °C.

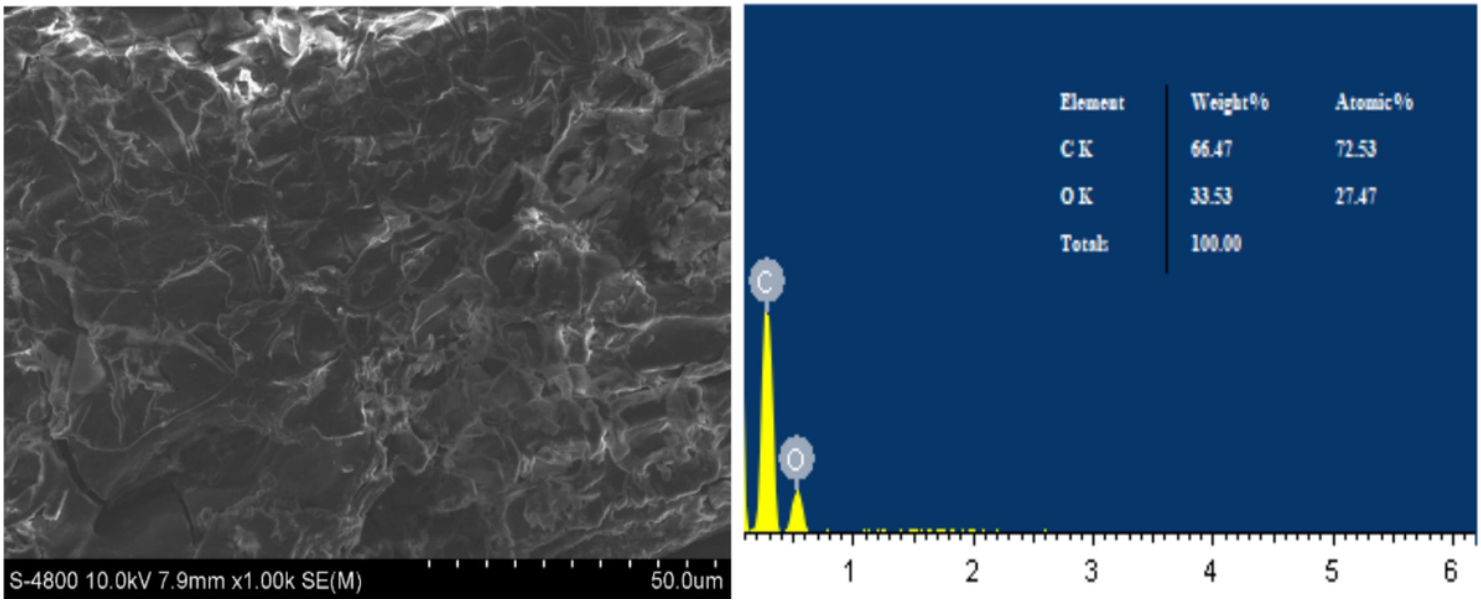

Figure 2

SEM and EDX analysis of pine leaves biomass

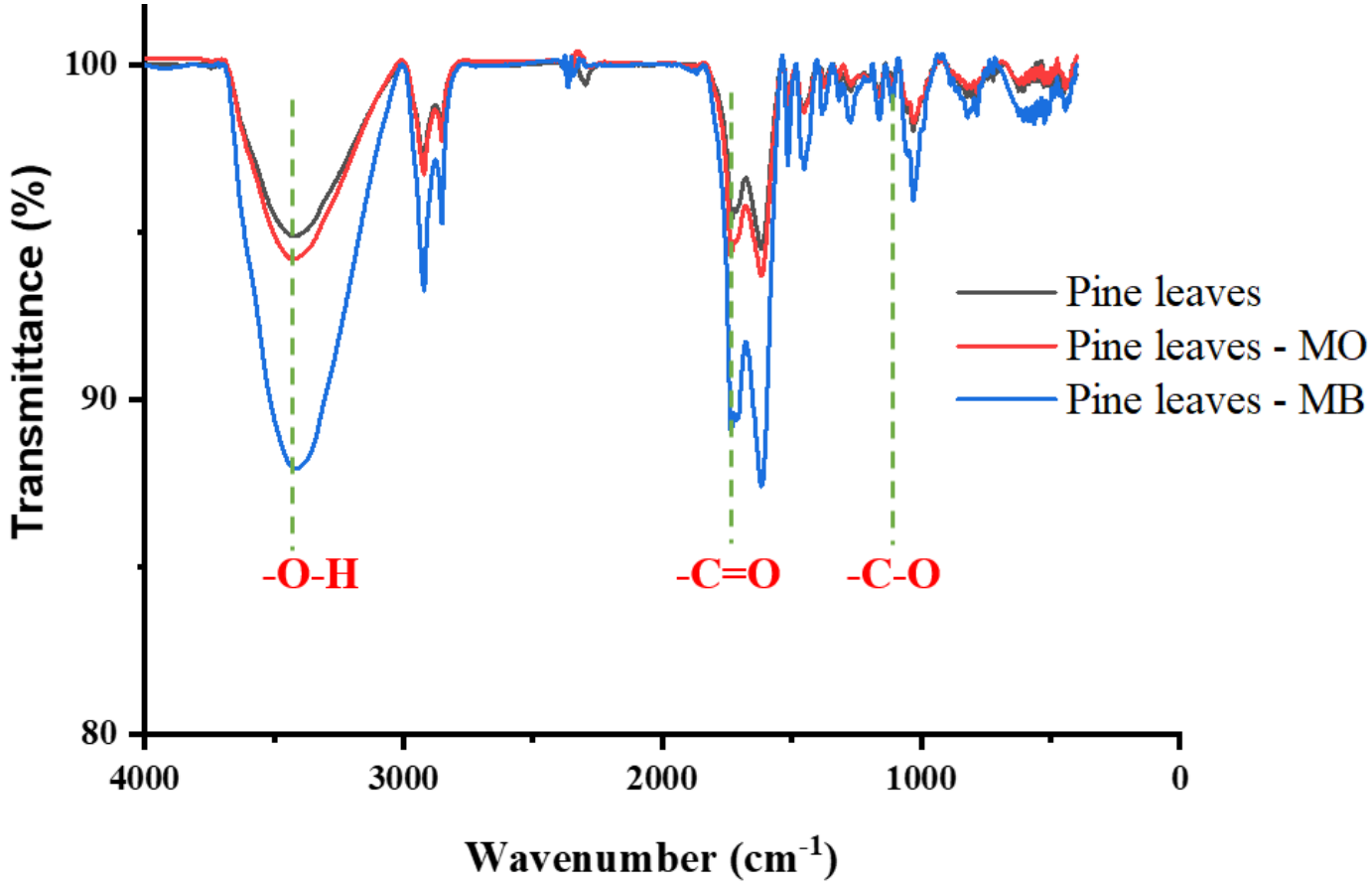

Figure 3

Comparative FT-IR spectra of Pine leaves before and after adsorption of dyes.

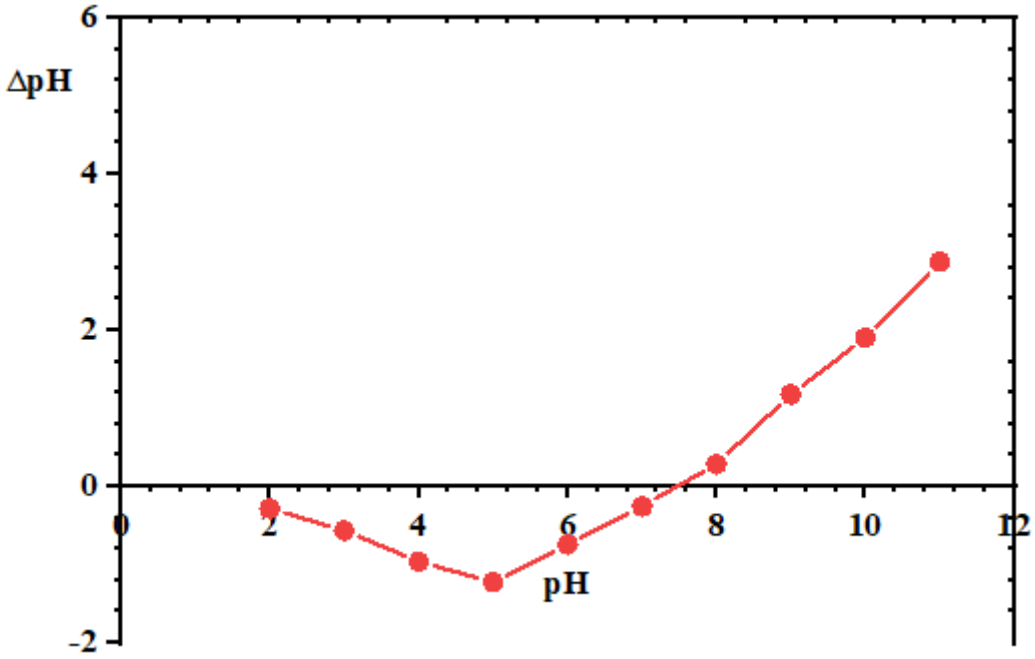

Figure 4

Determining the zero-charge point of material

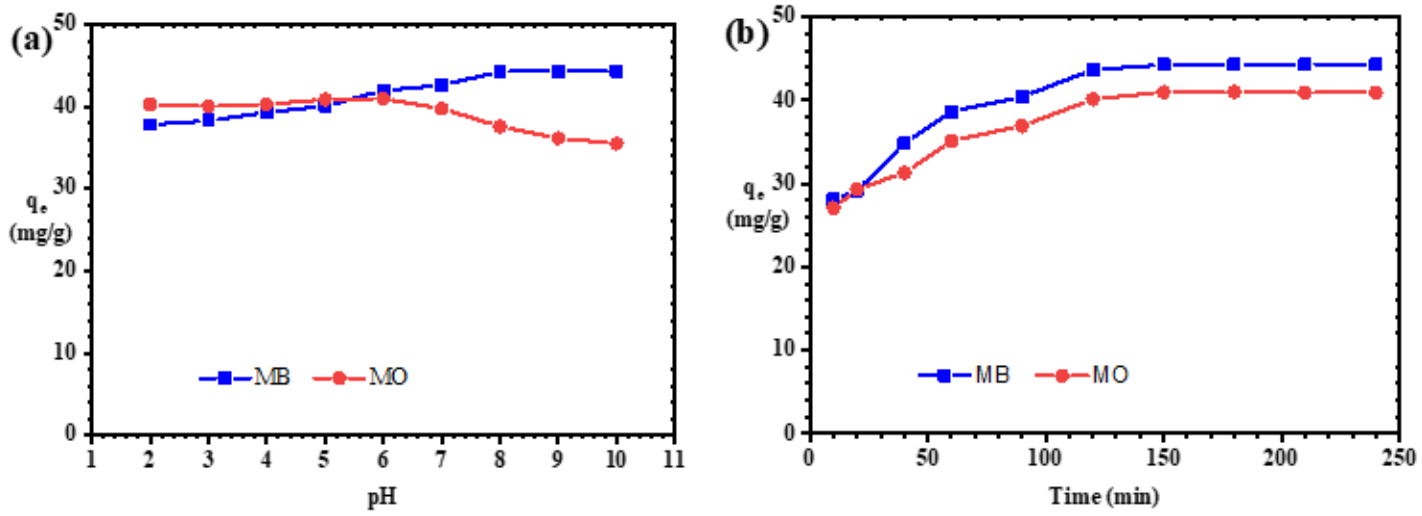

Figure 5

Effects of initial $pH_{solution}$ (a) and contact time (b) on MB and MO adsorption of biomass (C_0=100 $mg.L^{-1}$, dosage=0.1 g, and T=298 K)

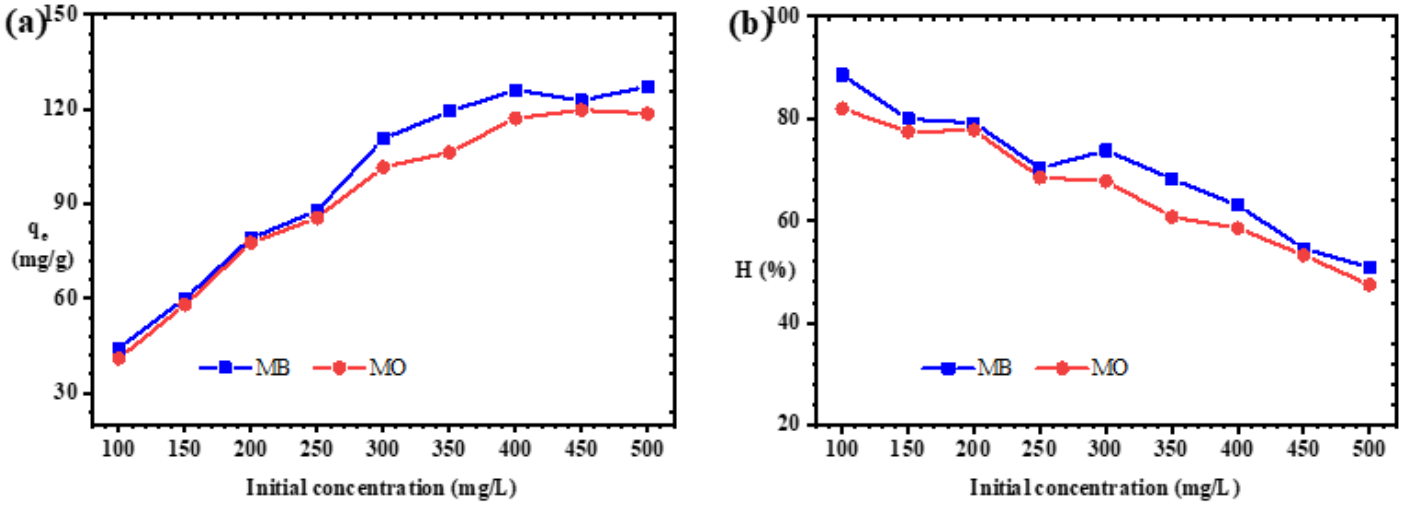

Figure 6

Effect of initial dyes concentration (pH_{MB} 8, pH_{MO} 6, contact time 150 minutes, dosage 0.1 g, and T 298 K) on the uptake of MB and MO of biomass

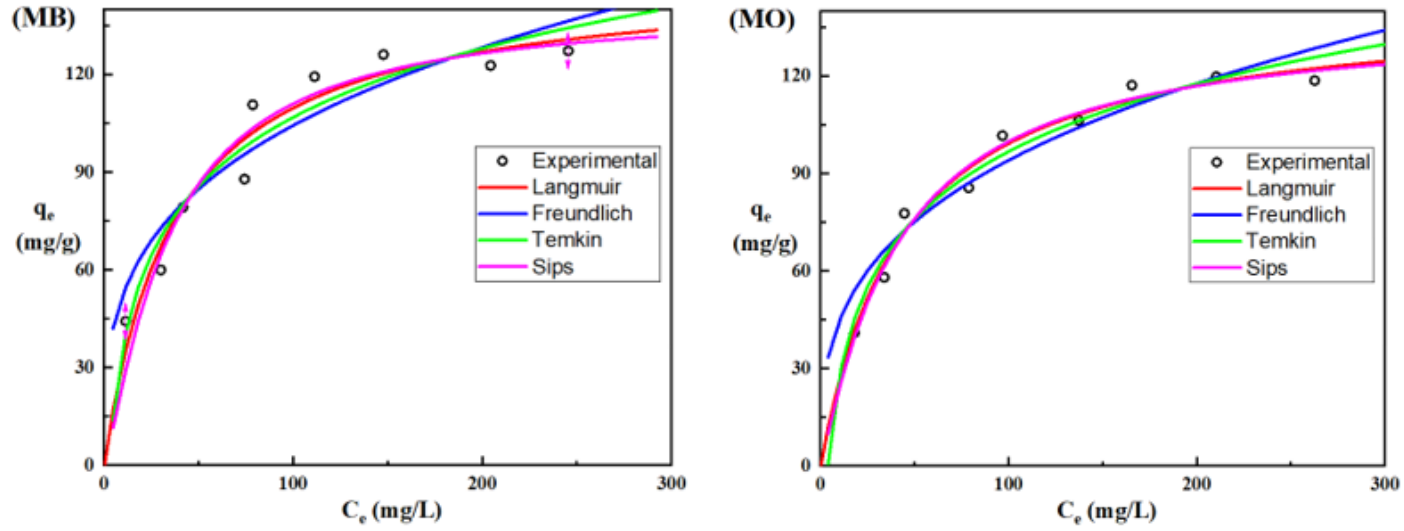

Figure 7

Fit of the Langmuir, Freundlich, Temkin and Sips isotherms of MB and MO adsorption onto biomass of Pinus kesiya

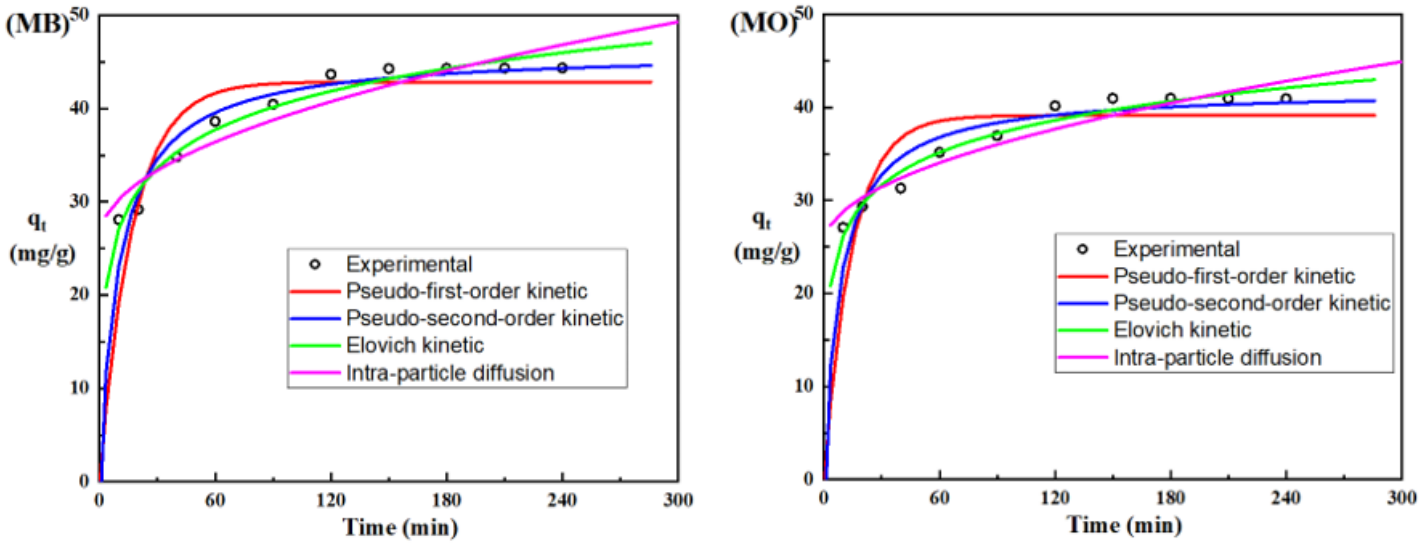

Figure 8

Fit of the MB and MO adsorption onto the biomass of Pinus kesiya using the pseudo-first-order, pseudo-second-order, Elovich, and intraparticle - diffusion kinetics models

Supplementary Files

This is a list of supplementary files associated with this preprint. Click to download.

- SupplementalInformation.docx